International Immunology, Vol. 20, No. 12, pp. 1527–1541
doi:10.1093/intimm/dxn112

Cryptococcus neoformans glucuronoxylomannan induces macrophage apoptosis mediated by nitric oxide in a caspase-independent pathway

Laura S. Chiapello, José L. Baronetti, Ana P. Garro, María F. Spesso and **Diana T. Masih**

Centro de Investigaciones en Bioquímica Clínica e Inmunología, CONICET, Departamento de Bioquímica Clínica, Facultad de Ciencias Químicas, Universidad Nacional de Córdoba, Medina Allende y Haya de la Torre, Ciudad Universitaria, 5000 Córdoba, Argentina

Keywords: apoptosis-inducing factor, CD18, FcγRII, mitochondria, PKC

Abstract

Glucuronoxylomannan (GXM) is the major component of *Cryptococcus* capsular polysaccharide, which represents an essential virulence factor for this yeast. *Cryptococcus neoformans* infections in immunocompetent rats are associated with inducible nitric oxide synthase (iNOS) expression and nitric oxide (NO) production by macrophages. This study demonstrates *in vitro* and *in vivo* that GXM promotes iNOS expression with NO production in rat macrophages. GXM also induced macrophage apoptosis after 48 h of culture, with this phenomenon being prevented by the iNOS inhibitor, aminoguanidine. The NO-induced macrophage apoptosis triggered by GXM was dependent on interactions with CD18, Fcγ receptor II and protein kinase C activation, without participation of tyrosine kinases or mitogen-activated protein kinases. Furthermore, this study reveals that GXM down-regulates the macrophage caspase-3 activity, induces a caspase-independent cell death and promotes depolarization of mitochondria membrane potential with increased cytosolic expression of the apoptosis-inducing factor. Taken together, this study describes the pathways and mechanisms involved in the macrophage apoptosis promoted by GXM through NO generation. These findings indicate new mechanisms of immunomodulation for the main capsular polysaccharide of *C. neoformans.*

Introduction

Cryptococcus neoformans is a facultative intracellular pathogen that causes severe meningoencephalitis or disseminated mycosis in immunocompromised patients (1, 2). This encapsulated yeast is also able to persist in healthy hosts, thus causing dormant infections that latter may reactivate under immunosuppressive disease (3). Cryptococcal infections in rats have been shown to have similarities with human cryptococcosis, revealing a strong granulomatous response and a low susceptibility to disseminated infections (4).

As an important part of innate immunity, inducible nitric oxide synthase (iNOS or NOS2) is induced in macrophages in numerous diseases related to pathogenic micro-organisms (5). Most bacteria, fungi and protozoan activate iNOS in macrophages after invasion or by releasing soluble LPSs or proteins (6–8). Several studies have revealed that nitric oxide (NO) could have a dual role during infections, with both anti-microbial effector functions and immunosuppressive properties mediated by the apoptosis of inflammatory cells (6, 9–11).

Apoptosis is a carefully regulated suicide program, which can be manipulated by pathogens, thereby representing one of the key factors in the survival strategy of micro-organisms (12). Apoptosis of activated macrophages has been recognized as a physiological and altruistic mechanism that helps to reduce the inflammatory stress (13). In this sense, the contribution of NO in triggering apoptosis in macrophages has been well established (11). Two pro-apoptotic signal transduction pathways have been described: an extrinsic/receptor-linked apoptotic pathway and an intrinsic/mitochondria-mediated pathway. Both activate downstream effector caspase-3, which leads to apoptosis features (14). However, mitochondrial damage can also lead to caspase-independent death through activation of death effectors, such as the apoptosis-inducing factor (AIF) or endonuclease G (Endo G) (15, 16).

The prominent anti-phagocytic polysaccharide capsule, which is comprised of glucuronoxylomannan (GXM), is

Correspondence to: D. T. Masih; E-mail: dmasih@fcq.unc.edu.ar

Received 16 May 2008, *accepted* 16 September 2008

Transmitting editor: K. Sugamura

Advance Access publication 16 October 2008

unique to *Cryptococcus* spp. and is considered to be an essential virulence factor that has multiple effects on host immunity (2). This acidic and viscous polysaccharide is continuously released by encapsulated yeasts during their replication, with high levels of GXM in the body fluids of patients with cryptococcosis having a direct relationship on the severity of disease (17, 18). Several publications have demonstrated that GXM interactions with CD14, CD18, Toll-like receptor (TLR)-4 or Fcγ receptor II (FcγRII) on phagocytic cells interfere with antigen presentation, promote L-selectin shedding, up-regulate the Fas ligand and co-stimulatory molecule expression and also modulate cytokine synthesis (19–23). Furthermore, GXM promotes nuclear factor-kappa B (NF-κB) translocation into the nucleus of RAW 264.7 cells, but does not lead to stimulation of mitogen-activated protein kinase (MAPK) pathways (19). However, it has also been described that GXM accumulation in murine macrophages depends on protein kinase C (PKC), tyrosine kinases and phospholipase C activation (24).

Previous studies have demonstrated that the control of pulmonary or disseminated cryptococcosis in immunocompetent rats is associated with the iNOS expression and NO production by macrophages (9, 25). However, there is little knowledge about how purified *C. neoformans* capsular polysaccharide modulates iNOS expression or NO production by macrophages (26, 27). Furthermore, we have previously reported apoptosis of tisular macrophages during a model of disseminated cryptococcosis, and we have also detected TdT-mediated biotin–dUTP nick-end labeling (TUNEL)-positive cells in tissues after intracardiac (i.c.) inoculation of GXM in rats (28–30). *In vitro* studies from our laboratory and others have demonstrated that GXM induces apoptosis of rat splenocytes (28), activated human T cells (22) and murine macrophages (27).

Taking everything mentioned above into account, the aim of this study was to investigate the ability of GXM to induce iNOS expression and NO production in rat macrophages, thereby revealing the role of this metabolite on the GXM-mediated apoptosis. The data presented here demonstrate that GXM promotes NO-dependent macrophage apoptosis and also provide evidence about the receptors and signaling pathways involved in these phenomena.

Methods

Reagents and media

For cell cultures, RPMI 1640 supplemented with 10% fetal bovine serum (FBS), 2 mM glutamine and 50 mg ml^{-1} gentamycin (Sigma–Aldrich Co., St Louis, MO, USA) was used. Tyrosine kinase inhibitor (genistein), PKC inhibitor (staurosporine), iNOS inhibitor [aminoguanidine (AG)], polymixin B (PB), mannan, laminarin and LPSs were obtained from Sigma–Aldrich. p-38 MAPK (SB203580) and MAPK/extracellular signal-regulated kinases (ERK) (PD98059) inhibitors were obtained from InvivoGen (San Diego, CA, USA). Mouse mAb to rat CD32 (FcγRII), CD11b/c and CD18 were obtained from BD Biosciences (San Jose, CA, USA). Antibodies to TLR-2, TLR-4, rabbit polyclonal antibody directed to iNOS or AIF, secondary antibodies and the pan-caspase inhibitor, N-Benzyloxycarbonyl-Val-Ala-Asp(O-Me) fluoromethyl ketone (Z-VAD-fmk), were purchased from Santa Cruz Biotechnology (Santa Cruz, CA, USA). Apoptosis Detection Colorimetric Biogene Kit was purchased from US Biological (United States Biological, MA, USA). Tetramethylrhodamineethylester (TMRE) was obtained from Molecular Probes (Eugene, OR, USA).

GXM-specific antibody 2H1 (mouse IgG1) was a generous gift from Arturo Casadevall (Albert Einstein College of Medicine, Bronx, NY, USA).

Micro-organism and cryptococcal polysaccharide

GXM was obtained from serotype A *C. neoformans* strain 102/85 (National University of Cordoba stock culture collection), serotype A *C. neoformans* strain 15 [62067; American Type Culture Collection (ATCC)] and serotype B *Cryptococcus gattii* strain NIH 112B. *Cryptococcus neoformans* strain 102/85 is a clinical isolate with a large capsule typified by phenotypic analysis and PCR multiplex, which was used in previous studies (9, 28–30). GXM was isolated following a streamlined method described by Cherniak *et al.* (17) with slight modifications. Briefly, *C. neoformans* isolates were expanded in 200 ml of a chemically defined liquid medium. After 5 days in a gyratory shaker at 30°C, the culture was autoclaved for 15 min at 121°C, and the cells were removed by centrifugation (18 000 × *g*) for 1 h. In order to neutralize the bacterial LPS contamination, 10 μg ml^{-1} of PB was added to the culture supernatant, which was then adjusted to 0.2 M NaCl, and 0.25 g of cetyltrimethyl ammonium bromide (CTAB) was added to the stirred solution. Two volumes of a 0.05% solution of CTAB were added slowly, and the precipitate was recovered by centrifugation (5000 × *g*) for 15 min. The pellet was then dissolved in 1 M NaCl by stirring overnight. GXM was precipitated by the slow addition of three volumes of 95% ethanol and kept overnight at 4°C. The polysaccharide was recovered by centrifugation (3000 × *g*) for 20 min at 4°C, dissolved by stirring overnight in 1 M NaCl and dialyzed against both 1 M NaCl and then milliQ H_2O for 1 week. The polysaccharide preparation was filtered through a Millipore MILLEX-HV 0.45-μm pore size filter (Millipore, Ireland), lyophilized and then re-suspended in saline solution at 2 mg ml^{-1}. This concentration of GXM was checked by the phenol–sulfuric acid method (31) and latex agglutination (Latex-Crypto Antigen Detection System; Immuno-Mycologics). The purity of GXM preparations was tested by 1H nuclear magnetic resonance (17). A 250 μg ml^{-1} sample from the GXM preparation had <0.03 endotoxin units per milliliter of endotoxin as measured by the Limulus Amebocyte Lysate assay (E-TOXATE®; Sigma–Aldrich).

Fluorescein-labeled GXM was prepared by binding the polysaccharide to FITC following a method described by Prigent-Richard *et al.* (32). Briefly, FITC and GXM were dissolved in a 0.1 M borate buffer solution at pH 9. The reaction was allowed to react overnight at room temperature with gentle stirring. FITC–GXM was separated from free FITC by extensive dialysis for 1 week. Then, FITC–GXM was filtered, lyophilized and re-suspended in saline solution at 2 mg ml^{-1}.

Isolation and culture of rat peritoneal macrophages

Female Wistar rats (7–8 weeks old), weighing 250 g, were housed and cared for in the animal resource facilities of the

Department of Clinical Biochemistry, Faculty of Chemical Sciences, National University of Cordoba, according to the institutional guidelines. Animals were sacrificed following protocols approved by the Animal Experimentation Ethics Committee, Faculty of Chemical Sciences, National University of Cordoba. Resident peritoneal cells were obtained by lavage of the peritoneal cavity with 45 ml of ice-cold PBS containing 0.1% FBS. Macrophages were separated from other cell populations using a discontinuous Percoll gradient (33). Briefly, peritoneal cells were centrifuged at 1500 r.p.m. for 10 min, re-suspended in 2 ml of HBSS and slowly added to the Percoll gradient (2 ml of a solution of Percoll with a density of 1.090 g ml^{-1} and 2 ml more but with a density of 1.080 g ml^{-1}, carefully overlaid). Tubes were centrifuged at 1500 r.p.m. for 30 min, and macrophages were collected from the interface between the Percoll layers. After being washed twice in RPMI 1640, cells were cultured in RPMI 1640 with FBS 10% for 6 h at 37°C in 5% CO_2. Adherent cells were harvested and re-suspended in RPMI supplemented with 10% FBS. Cell viability was >95% as determined by using trypan blue exclusion. May-Grünwald–Giemsa staining showed >90% of cells to have a macrophage morphology, and flow cytometry analysis revealed ~98% $CD11b/c^+$, 97% $MCHII^+$ and 65% $ED2^+$ cells.

For the measurement of nitrites, macrophages were incubated in a 24-well plate with 10^6 cells per well in 1 ml of supplemented RPMI in the absence (controls) or presence of varying GXM concentrations, for 24 or 48 h at 37°C in a 5% CO_2 humidified atmosphere. In some experiments, the cultures were performed in the presence of PB (5–50 μg ml^{-1}), AG (2 mM), staurosporine (0.5, 1 or 1 μM), genistein (5, 10 or 20 μM), PD98059 (10, 20 or 40 μM), SB203580 (5, 10 or 20 μM), anti-CD11b/c (10 μg ml^{-1}), anti-FcγRII (10 μg ml^{-1}), anti-CD18 (10 μg ml^{-1}), anti-TLR-2 (10 μg ml^{-1}), anti-TLR-4 (10 μg ml^{-1}), mannan (3 mg ml^{-1}), laminarin (3 mg ml^{-1}) or LPS (5 or 10 μg ml^{-1}).

For western blot analysis, macrophages (10^6 cells ml^{-1}) were cultivated for 48 h in 6-cm dishes in the absence or the presence of GXM (250 μg ml^{-1}), AG (2 mM), LPS (10 μg ml^{-1}) or staurosporine.

Nitrite measurement

Nitrite accumulation, an indicator of NO production, was measured using the Griess reagent (9). Briefly, 100-μl aliquots of 24- or 48-h culture supernatants were mixed with an equal amount of Griess reagent and incubated at room temperature for 15 min. The absorbance at 540 nm was measured using an automated microplate reader (Bio-Rad, CA, USA). The concentration of nitrite was calculated from a $NaNO_2$ standard curve.

SDS-PAGE and western immunoblotting

Cytosolic iNOS or AIF was detected as previously reported (34) from macrophage cultures performed as described above. Macrophages were harvested by washing several times with ice-cold PBS and scrapping. These were then washed twice in cold PBS and incubated for 30 min on ice in a buffer containing 20 mM HEPES (pH 7.5), 250 mM sucrose, 10 mM KCl, 1.5 $MgCl_2$, 1 mM EDTA, 1 mM dithiothreitol, 1 mM phenylmethylsulfonyl fluoride, 2 μg ml^{-1} leupeptin, 10 μg ml^{-1} aprotinin and 2 μg ml^{-1} pepstatin. The cells were disrupted at 4°C by 40 passages through a 27-gauge needle fitted in a 1-ml syringe and centrifuged at 700 × *g* for 15 min. The supernatant was transferred to an Eppendorf tube and was further cleared by centrifugation at 30 000 × *g* for 20 min at 4°C. The protein content was determined by a standard Bradford protein assay (Bio-Rad) and an equal amount of protein was separated on a 10% SDS-PAGE before being electrophoretically transferred to nitrocellulose paper, with the protein transfer being confirmed by Ponceau S staining. The blots were blocked with 5% milk in Tris buffered saline-Tween 20 for 1 h and then incubated overnight at 4°C with anti-iNOS, anti-AIF, anti-α-tubulin or anti-β-actin antibodies (Santa Cruz Biotechnology). Protein detection was done with a goat anti-rabbit IgG-HRP (sc2054; Santa Cruz Biotechnology) and developed using enhanced chemiluminescence detection reagents (Amersham Biosciences, NJ, USA) with autoradiographic or maximum performance light films (Kodak, NY, USA).

Macrophage nitrite production after intra-peritoneal GXM treatment of rats

Rats were intra-peritoneally (i.p.) inoculated with physiological solution, LPS (500 μg) or GXM (5 mg). Then, 12 h after injection, peritoneal macrophages were collected, and NO production was measured as nitrite levels in supernatants after 48 h of culture in the absence or the presence of AG or staurosporine. Three animals per group were used for these experiments. The dose of GXM for rat inoculation was chosen by taking into account that a mean of 20 × 10^6 macrophages from the peritoneal cavity of a normal rat was usually obtained, after Percoll purification. In this way, we tried to reproduce *in vivo* the ratio of GXM/macrophage tested in experiments performed *in vitro* namely: 250 μg of GXM per 1 × 10^6 macrophages.

In vivo iNOS expression in lung tissue after i.c. GXM treatment of rats

As we previously reported (30), rats were injected via the i.c. route with 500 μg of GXM. Then, 7 days after inoculation, rats were anesthetized before being killed. Lungs were then removed and fixed in formalin. Saline-treated rats were used as negative controls. iNOS was detected in tissue sections by immunohistochemistry using anti-iNOS antibody (1/50; Santa Cruz Biotechnology) and goat anti-rabbit IgG-HRP (1/100; Santa Cruz Biotechnology) as the secondary antibody. Color was developed with diaminobenzidine (DAB), and the tissue was counterstained with hematoxylin. Negative controls consisting of the primary antibody omission and the staining of tissues from saline-treated rats were also carried out.

Intracellular detection of GXM in macrophages

Macrophages were cultivated in a 24-well plate as described above, in the absence or the presence of GXM (50 and 250 μg). After 12 h of culture, cells were scraped and washed with ice-cold PBS. For intracellular GXM detection (35), cells were then thoroughly washed with PBS for removal of unbound

GXM, fixed in 4% PFA and permeabilized with 1% triton X-100. After being washed twice with PBS, cells were blocked for 30 min in 1% human serum albumin in PBS and incubated with the anti-GXM antibody 2H1 (3 μg ml^{-1}) for 1 h at room temperature, followed by staining with a rat anti-mouse FITC-conjugated secondary antibody (BD Biosciences). Cells were then analyzed by flow cytometry (Cytoron Absolute; ORTHO Diagnostic System) or fluorescence microscopy in cytospin preparations. In a similar way, cytospin preparations of freshly explanted peritoneal macrophages from rats injected with physiological solution or GXM (5 mg) for 12 h were fixed, permeabilized, immunostained for GXM detection and analyzed by fluorescence microscopy. Furthermore, immunochemical detection of GXM was performed in cytospin preparations following the method described above, but with endogenous peroxidase being neutralized by the incubation of cells with 2% hydrogen peroxide for 30 min before blocking. Peroxidase-conjugated goat anti-mouse IgG (Sigma–Aldrich) was applied as a secondary antibody and color was developed with DAB (Sigma–Aldrich). Cytospin preparations of macrophages were counterstained with hematoxylin.

Flow cytometry analysis of GXM accumulation in rat macrophages

Macrophages (10^6) were incubated with 250 μg of GXM–FITC for 12 h at 37°C in 5% CO_2, in the absence or presence of anti-CD18 (10 μg ml^{-1}), anti-FcγRII (10 μg ml^{-1}), anti-CD11b/c, mannan (3 mg ml^{-1}), laminarin (3 mg ml^{-1}), anti-TLR-2 (10 μg ml^{-1}), anti-TLR-4 (10 μg ml^{-1}), staurosporine (1 μM), genistein (10 μM), SB203580 (10 μM) or PD98059 (20 μM). These blocking antibodies or chemical inhibitors were added to the cultures 1 h before GXM–FITC. After incubation, the cells were collected by centrifugation, fixed in 2% PFA, washed three times with flow wash and analyzed by flow cytometry (Cytoron Absolute; ORTHO Diagnostic System). The mean fluorescence intensity (MFI) of labeled cells was determined using logarithmic-scale histograms. Autofluorescence was assessed using untreated cells. As control, macrophages were pre-incubated with unlabeled GXM and then GXM–FITC was added. Pre-incubation of the cells with 250 μg of unlabeled GXM nearly completely canceled out the increase in MFI observed following incubation with GXM–FITC (data not shown).

Apoptosis

Macrophages (1×10^6 ml^{-1}) were incubated in medium alone or with GXM (250 μg ml^{-1}). Then, 48 h after culture, apoptosis was detected in cytospin preparations stained with May-Grünwald–Giemsa by typical morphological changes (36). Apoptotic nuclei were revealed by fluorescence microscopy using a TUNEL kit (Boehringer Mannheim, Inc., USA) according to the manufacturer's protocol (28, 30). In addition, macrophages treated or untreated with GXM were pre-incubated with AG (2 mM), staurosporine (1 μM), genistein (10 μM), anti-CD11b/c (10 μg ml^{-1}), anti-FcγRII (10 μg ml^{-1}), anti-CD18 (10 μg ml^{-1}) antibodies or the pan-caspase inhibitor Z-VAD-fmk (10 μM). Then, the percentage of hypodiploid DNA was evaluated by flow cytometry after staining ethanol-fixed cells with propidium iodide (PI, 50 μg ml^{-1}) as described by Nicoletti *et al.* (37). Alternatively, apoptotic cells were labeled with FITC-conjugated annexin V (Santa Cruz Biotechnology) by simultaneous application of PI staining on unfixed cells (38) and then analyzed by flow cytometry.

Measurement of caspase activity

Caspase-3 activity was measured by an Apoptosis Detection Colorimetric Biogene Kit (US Biological). In this kit, DEVD-*p*-nitroanilide (pNA) is included as a substrate for caspase-3. Macrophages (1×10^6 ml^{-1}) were cultured in medium alone or with GXM (250 mg ml^{-1}). After 24, 48 and 72 h in culture, the cells were washed twice with PBS, sedimented by centrifugation and re-suspended in 50 ml of lysis buffer. The cell lysate was then incubated on ice for 15 min before being centrifuged at 10 000 r.p.m. for 10 min. Then the supernatants were collected and transferred to a 96-well microtiter plate. The protein concentration was measured by the Bradford method, and all the samples were standardized to the same amount of proteins. After that, 50 ml of reaction buffer (containing 10 mm ditiotreitol) and 5 ml of substrate (4 mM) were added. This reaction mixture was then incubated at 37°C for 3 h, and the formation of pNA was measured every hour at 405 nm using a microtiter plate reader. Results expressed as Δ caspase-3 activity were calculated by subtracting the optical density measured at 405 nm at T_0 from the optical density at 2 h after reaction (39).

Mitochondrial depolarization

The mitochondria-specific dye, TMRE, was used to measure mitochondrial potential changes ($\Delta\psi_m$) occurring during apoptosis (40). After 48 h of culture, macrophages (10^6 ml^{-1}), untreated or treated with GXM (250 μg ml^{-1}), were re-suspended in complete medium and incubated with 50 nM of TMRE (Molecular Probes) for 20 min at 37°C. At the end of incubation, cells were washed in HBSS, re-suspended in the flow analysis buffer (PBS with 0.2% FBS) and kept on ice until analysis by flow cytometry. The MFI of labeled cells was determined using logarithmic-scale histograms.

Statistical analysis

Three animals per group were used in all studies, with experiments being performed in triplicate on samples of individual animals from each group. The mean and SEM values were compared using the Student's *t*-test. Values of $P < 0.05$ were considered significant.

Results

GXM stimulates iNOS expression and NO production in rat macrophages

Macrophages were incubated for 48 h with varying concentrations of GXM or LPS as the positive control, in the absence or presence of AG, a specific inhibitor of iNOS. As shown in Fig. 1(A), GXM was able to stimulate macrophage NO production in a dose-dependent manner, with 250 μg of polysaccharide inducing a 2- or 3-fold increase in nitrite levels with respect to controls. GXM also induced iNOS expression, which was detected in the cytosol of

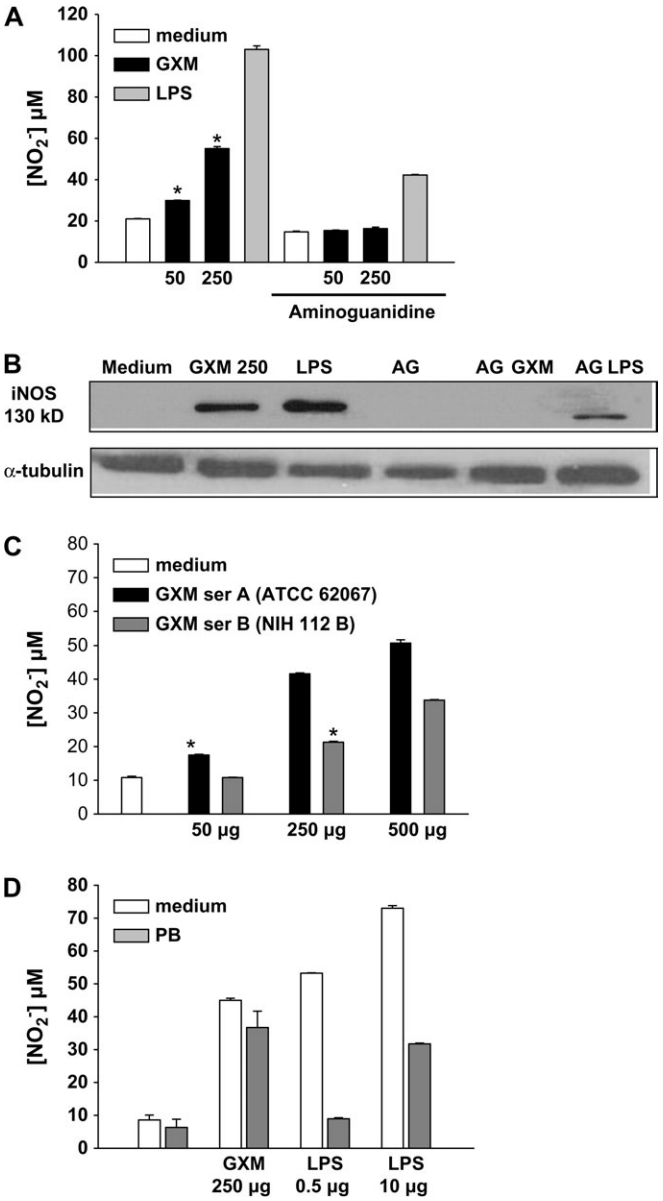

Fig. 1. GXM induces NO production and iNOS expression by rat macrophages. Macrophages (10^6 ml^{-1}) were incubated for 48 h in medium alone or treated with GXM (50 or 250 µg ml^{-1}) or LPS (10 µg ml^{-1}) in the absence or presence of AG. (A) Nitrite levels were determined by Griess reaction in supernatants of cultures. *$P < 0.05$ (GXM 50 µg-treated versus -untreated cells; GXM 250 µg-treated versus GXM 50 µg-treated cells). (B) Western blot analysis using a specific antibody to iNOS or α-tubulin of cytoplasmic extracts from whole-cell lysates. Each lane was loaded with 30 µg of the cytosolic protein, and the protein content after transfer was tested by Ponceau S staining. Blots are representative of results from three separate experiments. (C) Dose-dependent nitrite production by macrophages incubated with GXM (50, 250 or 500 µg ml^{-1}) from *Cryptococcus neoformans* serotype A (ATCC 62067) or *C. gattii* serotype B (NIH 112B). *$P < 0.05$ (serotype A GXM 50 µg-treated versus -untreated cells; serotype B GXM 250 µg-treated versus -untreated cells). (D) Nitrite levels in supernatants of cultures from macrophages (10^6 ml^{-1}) incubated with medium alone, GXM (250 µg ml^{-1}) or LPS (0.5 and 10 µg ml^{-1}) in the absence or presence of PB (20 µg ml^{-1}). Bars represent the mean ± SEM of triplicates from three independent experiments.

cellular lysates by western blot (Fig. 1B). As expected, LPS induced high levels of nitrites or iNOS expression, with AG abrogating GXM-induced NO production or diminishing LPS-mediated NO synthesis.

We also tested if GXM samples isolated from serotype A *C. neoformans* ATCC 62067 or serotype B *C. gattii* NIH 112B strains also have the ability to stimulate nitrite production by rat macrophages. Figure 1(C) shows that GXM from ATCC 62067 serotype A also stimulated NO production to reach similar levels to those produced by the GXM isolated from our serotype A *C. neoformans* strain (Fig. 1A). However, GXM from serotype B *C. gattii* had a lower capacity than GXM from serotype A to stimulate nitrite production (Fig. 1C).

On the other hand, one of the main concerns about the GXM-mediated NO production by macrophages was the possibility that this effect could have been caused by the presence of bacterial LPS in GXM. To rule this out, we performed the experiments in the presence of different doses of PB (from 5 to 50 µg ml^{-1}). Figure 1(D) reveals that PB (20 µg ml^{-1}) did not abrogate the NO production induced by GXM. However, it did significantly suppress the levels of NO produced by macrophages stimulated with 0.5 or 10 µg of LPS. Furthermore, GXM induced NO synthesis in a dose-dependent manner, even in the presence of 40 µg of PB (data not shown). These results, in combination with our finding that GXM preparations were negative by the Limulus Amebocyte lysates assay, made it unlikely that the results attributed to GXM stimulation were actually due to LPS contamination.

Peritoneal macrophage nitrite production and lung iNOS expression from GXM-injected rats

We evaluated the ability of peritoneal macrophages from GXM-inoculated rats to produce NO after culture. To carry out these experiments, we took into account previous reports showing that the i.p. injection of bacterial LPS had promoted NO production by peritoneal cells after between 3 and 24 h following inoculation (41). Based on these data, rats were inoculated with physiological solution, LPS (500 µg) or GXM (5 mg). Then, 12 h later, peritoneal macrophages were collected and cultivated for 48 h. Figure 2(A) shows that macrophages from rats injected with physiological solution had a slight increase in nitrite levels compared with macrophages from untreated rats ($P < 0.05$). However, cells from GXM-treated rats produced higher nitrite levels than macrophages from saline-treated rats ($P < 0.005$). GXM (5 mg) stimulated similar levels of NO macrophage production to those induced by LPS (500 µg). In the presence of AG, macrophages from all groups of treated rats produced similar nitrite levels to those produced by untreated rats. Also, when a PKC inhibitor (staurosporine) was added to the cultures, the NO production was drastically suppressed by macrophages from GXM-treated rats, with no modification of the NO produced by macrophages from both saline-treated or -untreated animals. These results suggest the involvement of PKC activation in the GXM-mediated NO production. To a lesser extent, staurosporine also inhibited the nitrite produced by macrophages from LPS-inoculated rats. However, despite the presence of staurosporine in the

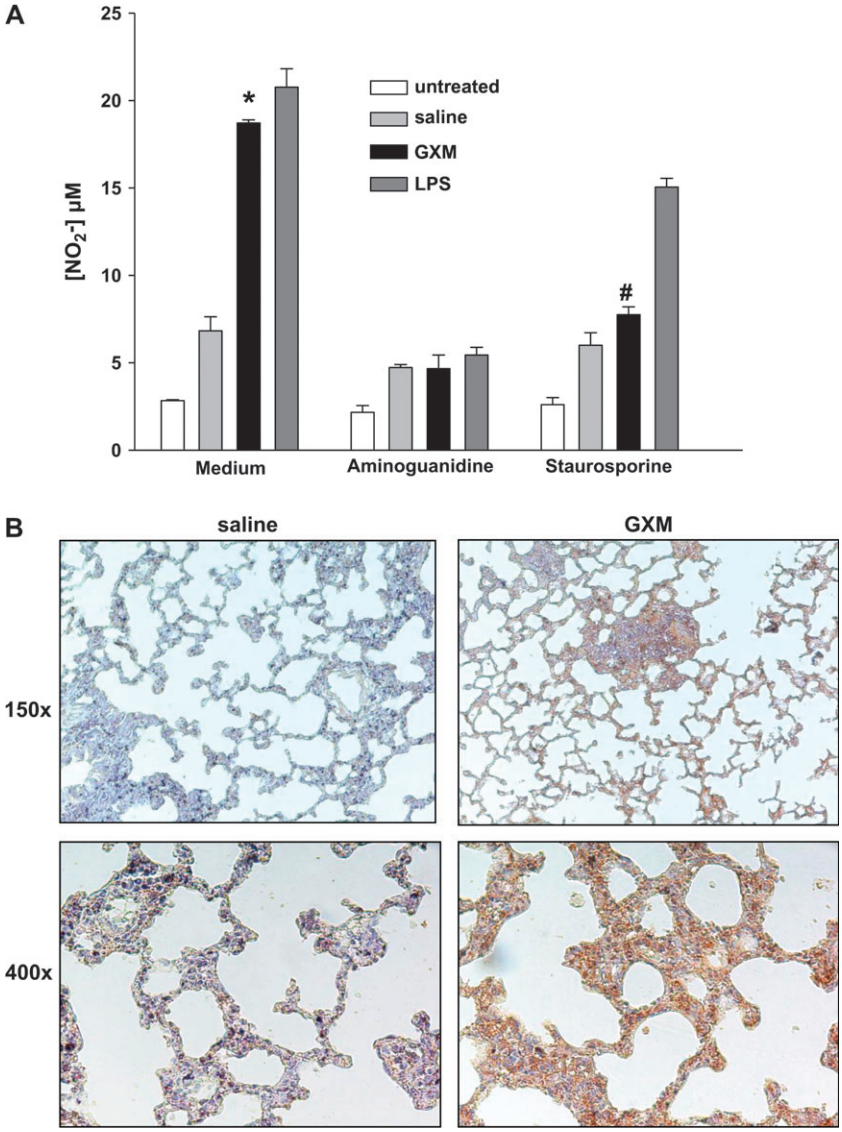

Fig. 2. Peritoneal macrophage nitrite production and lung iNOS expression in GXM-inoculated rats. (A) Nitrite levels after 48 h of culture of macrophages from rats untreated or i.p. injected with physiological solution (saline), LPS (500 μg) or GXM (5 mg) for 12 h. Peritoneal macrophages (10^6 ml^{-1}) from the different groups of animals were cultivated in the presence or absence of AG (2 mM) or staurosporine (1 μM). Bars represent the mean ± SEM of triplicates from two independent experiments. *$P < 0.05$ (GXM-injected rats versus saline-injected rats). #$P < 0.05$ (cells from GXM-injected rats incubated with staurosporine versus cells from GXM-injected rats in medium alone). (B) Micrographs of immunohistochemistry for iNOS (brown) in lung sections from 7-day inoculated rats via i.c. with physiological solution or GXM (500 μg). iNOS-specific rabbit polyclonal antibody and peroxidase-conjugated goat anti-rabbit IgG were used as primary and secondary antibodies. Color was developed with DAB–H_2O_2, and sections were counterstained with hematoxylin. Magnification ×150 and ×400.

culture, macrophages from LPS-treated rats released more NO than control animals ($P < 0.05$).

Furthermore, a previous publication from our laboratory demonstrated a strong immunohistochemical detection of GXM in sections of lungs from rats treated with GXM via the i.c. route (30). In the present study, we evaluated by immunohistochemistry, the *in vivo* iNOS expression in lung sections from GXM-treated rats via this route. As shown in Fig. 2(B), lung sections from rats treated with GXM (7 days) revealed stronger iNOS immunoreactivity compared with that observed in rats treated with physiological solution. Therefore, these data provide evidence that GXM not only promotes iNOS and NO production by macrophages *in vitro* but also stimulates NO *in vivo*.

CD18, FcγRII and PKC mediate GXM-induced NO production

Cryptococcus neoformans or GXM can either stimulate or suppress the functions of different types of cells through the interaction with mannose, glucans, FcγRII, CD11b/c, CD18 or TLRs (20–23, 42–44). To investigate the role of these receptors on GXM-induced NO production by macrophages, nitrite levels were evaluated in the presence of mannan, laminarin (which block mannose and B-glucan receptors, respectively) or blocking antibodies to FcγRII, CD11b/c,

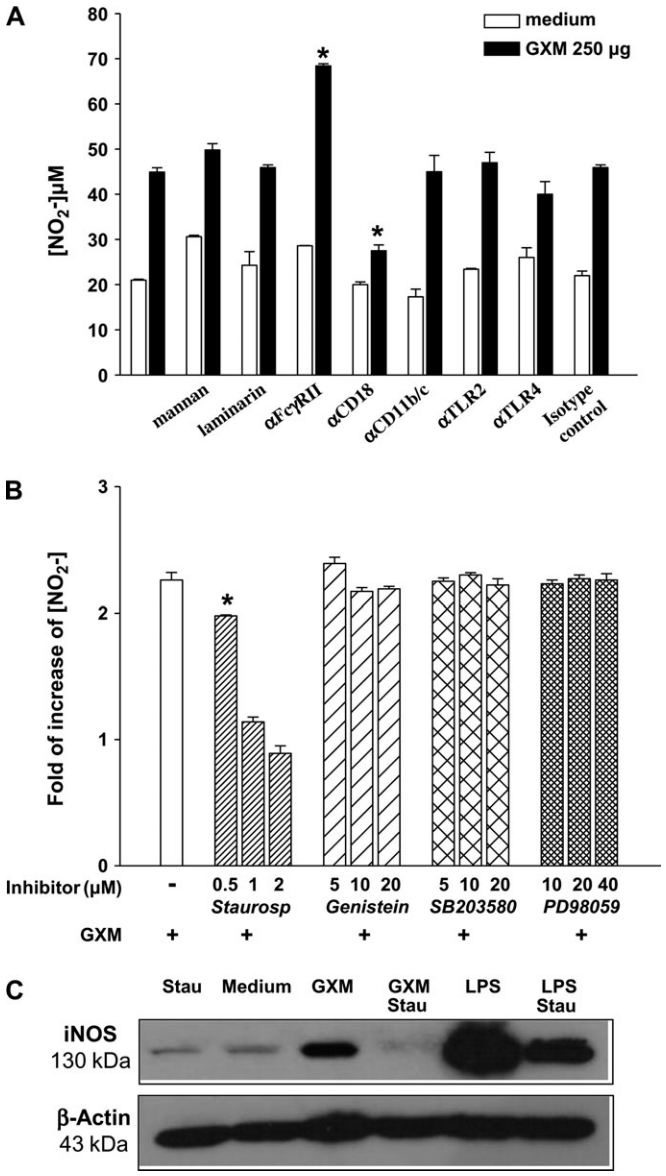

Fig. 3. Contribution of macrophage receptors and PKC, tyrosine kinases, p38 and ERK1/2 MAPK to the GXM-induced NO production. (A) Macrophages (10^6 ml^{-1}) were incubated in medium alone or treated with GXM (250 μg ml^{-1}) for 48 h in the absence or presence of mannan (3 mg ml^{-1}), laminarin (3 mg ml^{-1}), mAb to FcγRII (10 μg ml^{-1}), mAb to CD18 (10 μg ml^{-1}), mAb to CD11b/c (10 μg ml^{-1}), mAb to TLR-2 (10 μg ml^{-1}), mAb to TLR-4 (10 μg ml^{-1}) or isotype-matched control antibody (10 μg ml^{-1}). Nitrite levels were measured in culture supernatants by Griess reaction. (B) Fold of increase of nitrite levels of macrophages incubated for 24 h with GXM respect to those of macrophages in medium alone, in the presence or absence of staurosporine (0.5, 1 and 2 μM), genistein (5, 10 and 20 μM), SB203580 (5, 10 and 20 μM) or PD98059 (10, 20 and 40 μM). (C) Western blot analysis using a specific antibody to iNOS or β-actin of cytoplasmic extracts from whole-cell lysates. Macrophages (10^6 ml^{-1}) were incubated in medium alone or treated with GXM (250 μg ml^{-1}) or LPS (10 μg ml^{-1}) for 24 h in the absence or presence of staurosporine (1 μM). Blots are representative of results from two separate experiments. Bars represent the mean ± SEM of triplicates from three independent experiments. *$P < 0.05$ (GXM-treated cells pre-incubated with anti-CD18, anti-FcγRII antibodies or staurosporine versus GXM-treated cells).

CD18, TLR-2 or TLR-4. As shown in Fig. 3(A), neither mannan, laminarin nor blocking antibody to CD11b/c inhibited GXM-induced NO production. Similarly, antibodies to TLR-2 or TLR-4 did not suppress the GXM-induced NO. However, the presence of anti-FcγRII antibody in cultures increased NO synthesis by macrophages stimulated with GXM, without modifying the nitrite levels produced by macrophages incubated in medium alone. In contrast, the antibody directed to CD18 significantly suppressed GXM-mediated NO production. These data show that GXM signalizes via CD18 to stimulate NO synthesis by macrophages and suggest that interaction of GXM with FcγRII promotes inhibitory signals, which can then be reverted by blocking this receptor.

Expression of iNOS in rat macrophages is related to the activation of different intracellular signaling pathways (45). To assess the contribution of intracellular kinases in the GXM-induced NO synthesis, we evaluated the NO production in macrophages cultured for 24 h in the presence of inhibitors of PKC (staurosporine), tyrosine kinases (genistein), p38 MAPK (SB203580) and MAPK-ERK kinase (PD98059). The concentrations of chemical inhibitor used in these experiments, after 24 h of culture, did not modify macrophage viability. Furthermore, neither genistein nor staurosporine affected the nitrite levels of macrophages cultivated in medium alone, whereas PD98059 and SB203580 diminished the basal production of NO. For this reason, the results displayed in Fig. 3(B) are represented as fold of increase of nitrite level from macrophages treated with GXM, respect to those produced by macrophages in medium alone. According to the data presented in Fig. 2, these experiments demonstrate that the PKC inhibitor (staurosporine) abrogated NO production induced by GXM in a dose-dependent manner. However, neither the inhibitor of tyrosine kinases (genistein) nor the inhibitors of p38 or ERK1/2 MAPK (PD98059 and SB203580) modified the GXM-induced nitrite release by macrophages. Furthermore, staurosporine (1 μM) also inhibited iNOS expression levels of GXM or LPS-incubated macrophages without modifying the protein expression of macrophages in medium alone, which was detected by a high-sensitive light films in the western blot (Fig. 3C).

Based on these findings, we propose that activation of PKC, but not tyrosine kinases or p38 or ERK1/2 MAPK, is involved in GXM-dependent NO macrophage production.

CD18, FcγRII and PKC mediate GXM accumulation in rat macrophages

Purified GXM has been demonstrated to be efficiently phagocyted by mouse and human macrophages or dendritic cells (24, 35, 42). Here, we evaluated the *in vitro* and *in vivo* ability of rat macrophages to internalize GXM by detecting the polysaccharide in permeabilized cells by fluorescence microscopy or flow cytometry using the anti-GXM antibody 2H1. Figure 4(A) shows a significant loading of GXM after 12 h of culture, with ~85% of GXM-positive cells being found when cultures were performed with 50 or 250 μg ml^{-1} of GXM. However, the MFI of macrophages incubated with 250 μg of GXM was significantly higher with respect to the MFI of macrophages cultivated with 50 μg of GXM ($P < 0.05$, data not shown). In addition, the analysis of the GXM internalization

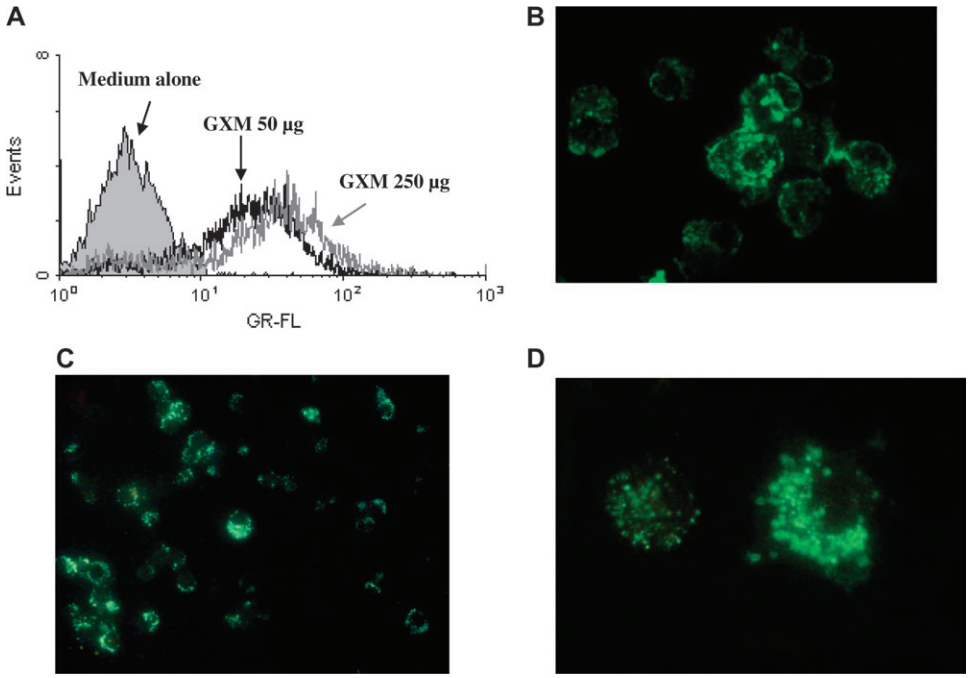

Fig. 4. GXM internalization by rat macrophages. Peritoneal macrophages (10^6 ml^{-1}) from normal rats were incubated in medium alone (shaded histogram), with GXM 50 µg ml^{-1} (black line open histogram) or GXM 250 µg ml^{-1} (gray line open histogram). After culture, cell suspensions or the cytospin preparation were fixed, permeabilized and then stained with the anti-GXM mAb 2H1, followed by labeling with FITC-conjugated secondary antibody and analysis by (A) flow cytometry or (B) fluorescence microscopy (GXM: 250 µg ml^{-1}. Magnification ×1000). (C and D) Representative micrograph of GXM immunofluorescence detection in freshly explanted peritoneal macrophages from rat injected with GXM (5 mg) for 12 h (×100 and ×1000, respectively).

by fluorescence microscopy showed a punctuate pattern of localization (Fig. 4B). Most macrophages from GXM-injected rats (12 h after i.p. injection of 5 mg of GXM) showed a positive reaction to GXM and also revealed a punctuate pattern of intracellular polysaccharide retention (Fig. 4C and D). The fluorescence reaction was negative in macrophages cultivated in medium alone, in peritoneal cells from rats injected with physiological solution or when the primary anti-GXM antibody was not used. Moreover, a weak fluorescence reaction was observed in fixed, unpermeabilized cells.

Next, we measured the ability of macrophages to bind GXM–FITC in the presence of blocking antibodies to cellular receptors or chemical inhibitors to intracellular kinases. Figure 5 shows that pre-incubation of macrophages with CD18- or FCγRII-blocking antibodies significantly inhibited GXM–FITC cell accumulation with respect to that observed in macrophages without blocking antibodies, after 12 h of culture (Fig. 5A and B). In contrast, the blocking of CD11b/c did not significantly modify GXM–FITC detection in macrophages (Fig. 5C). In a similar way, GXM–FITC detection in macrophages was not reduced in the presence of mannan, laminarin, blocking antibodies to TLR-2 or TLR-4 or isotype-matched control IgG (data not shown). In addition, the PKC inhibitor, staurosporine, was the only chemical inhibitor that significantly suppressed GXM–FITC accumulation in macrophages (Fig. 5D).

GXM induces NO-mediated macrophage apoptosis

We have demonstrated that GXM is able to induce apoptosis of rat splenocytes *in vitro* and to increase the level of tisular apoptosis *in vivo* (28–30). Thus, taking into account these previous reports together with the results presented in this study, we decided to investigate the effect of GXM on macrophage viability and the involvement of NO in GXM-mediated cell death. Figure 6(A) shows that macrophages cultured with 250 µg of GXM for 48 h revealed morphological features associated with apoptotic cell death, such as a decrease in cell size, a condensed chromatin and nuclei fragmented into small dense balls. In a similar way, Fig. 6(B) reveals macrophages with immunohistochemical detection of GXM and the morphological characteristics of apoptosis. Finally, Fig. 6(C) demonstrates cells with cytoplasmic immunofluorescence to GXM using mAb 2H1 and nuclei positive for TUNEL reaction.

To investigate the role of NO in GXM-mediated macrophage apoptosis, cells were incubated with GXM in the presence of AG. Then, apoptosis was measured by flow cytometry after ethanol fixation and PI staining or by annexin V–FITC binding of unfixed cells (Fig. 7A and B). GXM induced a significant increase in the percentage of cells with hypodiploid DNA, compared with macrophages in medium alone, after 48 h of culture (40.1 ± 2.2 versus 7.3 ± 0.8, $P < 0.05$). However, this phenomenon was completely abrogated in the presence of the iNOS inhibitor, AG. In a similar way, GXM increased the percentage of annexin V-positive cells with respect to controls ($P < 0.05$), with this effect being eliminated in the presence of the iNOS inhibitor. In addition, Fig. 7(C) reveals that the anti-CD18-blocking antibody or PKC inhibitor, staurosporine, inhibited

the apoptosis induced by GXM. Moreover, anti-FcγRII antibody increased the apoptosis induced by GXM, but anti-CD11b/c did not modify the levels of DNA subdiploid of macrophages incubated with the polysaccharide.

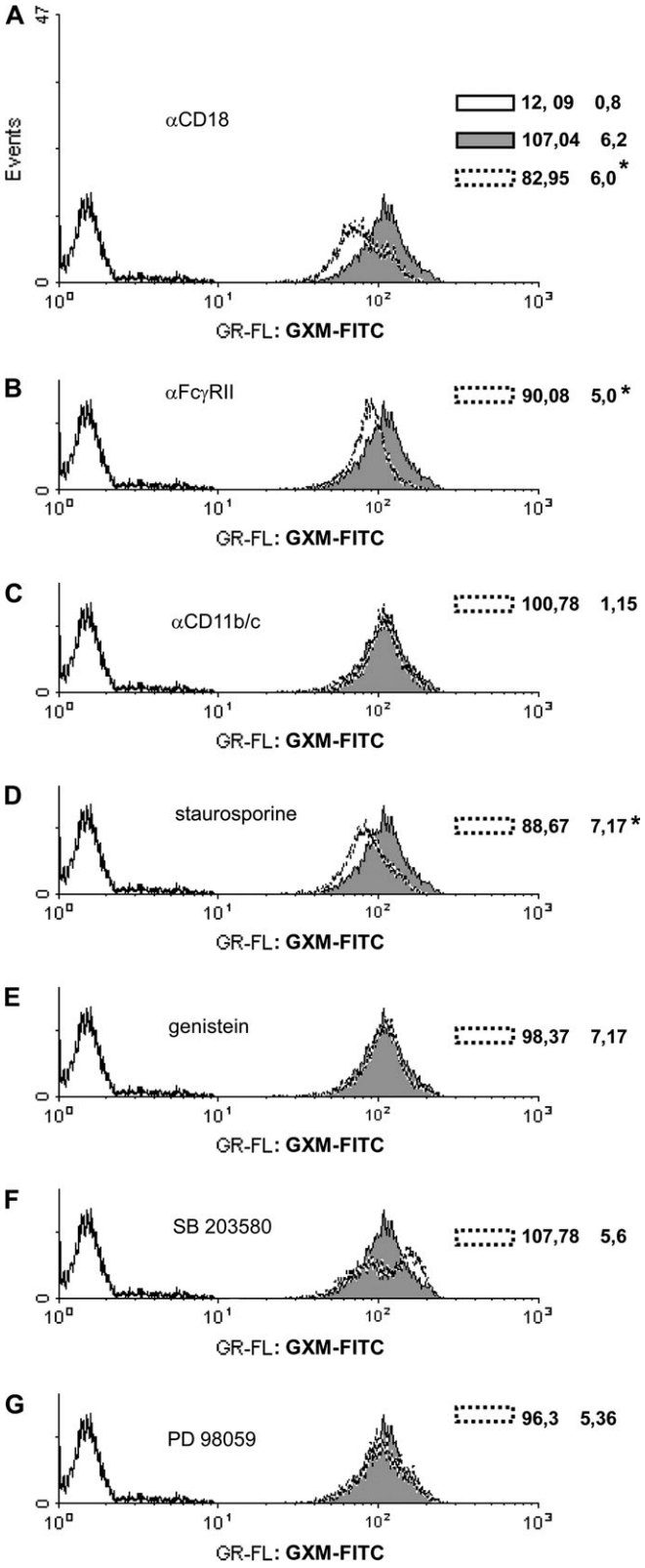

GXM induces macrophage apoptosis through a caspase-independent pathway with mitochondrial membrane depolarization and AIF release

Taking account that apoptosis is typically mediated by activation of the caspase cascade (14, 46), we measured the caspase-3 activity of macrophages in medium alone or incubated with GXM (250 μg) for 24, 48 or 72 h. Figure 8(A) shows that peritoneal macrophages in medium alone displayed enzymatic activity of caspase-3, which decreased with time of culture. However, the caspase-3 activity from macrophages incubated with GXM was even lower than that observed from controls. GXM suppressed the activity of caspase-3 from macrophages after 24, 48 or 72 h of culture, suggesting that apoptosis mediated by GXM is independent of caspase activation. To confirm this, we next measured the percentage of macrophage hypodiploid induced by GXM in the presence of the pan-caspase inhibitor Z-VAD-fmk. As shown in Fig. 8(B), the caspase inhibitor did not modify the levels of apoptosis induced by GXM. Instead, Z-VAD-fmk significantly increased the GXM-mediated apoptosis with respect to macrophages co-incubated with GXM in the absence of the inhibitor. Furthermore, we determined the NO involvement in the GXM-mediated caspase-3 activity suppression by performing cultures in the presence of the iNOS inhibitor, AG. Figure 8(C) shows that AG restored the caspase-3 activity from macrophages incubated with GXM ($P < 0.05$, GXM-treated cells in the presence of AG- versus GXM-treated cells).

Furthermore, mitochondrial damage can lead to caspase-dependent or caspase-independent apoptosis (47). The AIF is released from damaged mitochondria and is able to trigger a caspase-independent death pathway (47). Then, we performed experiments by flow cytometry using the mitochondria-specific dye, TMRE, in order to determine whether GXM induced changes in the mitochondrial membrane potential ($\Delta\psi_m$) (40). One representative analysis from three separate experiments is displayed in Fig. 9(A) and reveals that macrophages incubated with 250 μg of GXM had a significant decrease in TMRE mitochondrial retention compared with macrophages alone, after 48 h of culture (MFI: 51.72 ± 3.3 versus 35.01 ± 1.4; $P < 0.05$). In addition, western blot analysis of macrophage cytosolic extracts demonstrated that macrophages cultivated with 250 μg of GXM showed increased

Fig. 5. Contribution of cellular receptors and PKC, tyrosine kinases, p38 and ERK1/2 MAPK to GXM accumulation in macrophages. Macrophages (10^6 ml^{-1}) were incubated in medium alone or with FITC-labeled GXM (250 μg ml^{-1}) in the absence or presence of (A) anti-CD18 (10 μg ml^{-1}), (B) anti-FcγRII (10 μg ml^{-1}), (C) anti-CD11b/c (10 μg ml^{-1}), (D) staurosporine (1 μM), (E) genistein (10 μM), (F) SB203580 (10 μM) or (G) PD98059 (20 μM). After 12 h of incubation, the cells were fixed, washed three times and analyzed by flow cytometry. The MFI values of macrophages in medium alone (open histograms), with GXM–FITC (gray shaded histograms) or with GXM–FITC in the presence of blocking antibodies or chemical inhibitors (dotted line open histograms) are displayed in the right column of the figure. Histograms are representative of triplicates from two independent experiments. *$P < 0.05$ (GXM–FITC-treated cells in the presence of anti-CD18, anti-FcγRII or staurosporine versus GXM–FITC-treated cells).

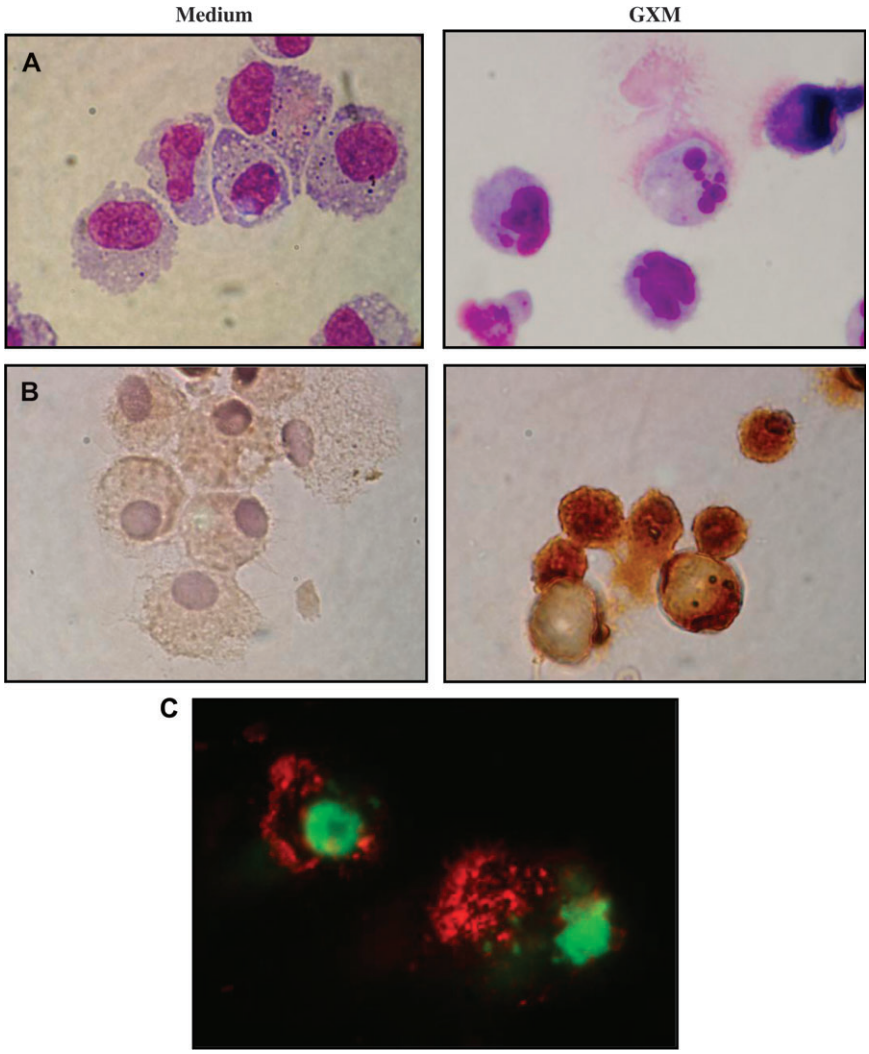

Fig. 6. GXM triggers apoptosis of rat peritoneal macrophages. Representative micrographs of cytospin preparations from macrophages (10^6 ml^{-1}) incubated for 48 h with medium alone (left) or GXM (250 μg ml^{-1}) (right). (A) May-Grünwald–Giemsa staining. (B) Immunohistochemistry for GXM using mAb 2H1 and peroxidase-conjugated goat anti-mouse IgG. Color was developed with DAB–H_2O_2 and cytospin counterstained with hematoxylin. (C) TUNEL (green nucleus) and immunofluorescence for GXM with mAb 2H1 and a PE-conjugated secondary antibody (red cytoplasm). All images were obtained at an original magnification of ×1000.

levels of AIF protein expression, in comparison with cytosolic extracts from cells incubated in medium alone (Fig. 9B).

Discussion

This study provides the first evidence that GXM from *C. neoformans* induces iNOS expression and NO by macrophages *in vitro* and *in vivo*, and this phenomenon triggers macrophage apoptosis. The data suggest that NO-mediated macrophage apoptosis induced by GXM occurs through polysaccharide interactions with CD18, FcγRII receptors and by PKC activation. Furthermore, the data presented here show that GXM suppresses caspase-3 activity and promotes a caspase-independent programmed cell death with alterations in the mitochondrial membrane integrity.

Macrophages can sense molecules derived from pathogens, which promotes iNOS activation with NO generation playing a central role in the innate immunity (5–7). Experiments performed with human astrocytes suggest that NO is an anti-cryptococcal effector molecule produced by human cells (48). Furthermore, previous studies from our laboratory, as well as others, have demonstrated elevated NO synthesis after iNOS expression by activated macrophages during rat cryptococcal infections (9, 25, 26). On the other hand, GXM is actively shed as a soluble exopolysaccharide during *Cryptococcus* replication, and GXM interactions with macrophages from humans, mice or rats exert different immunobiological effects (44). Herein, we have demonstrated that the interaction of purified capsular polysaccharide, GXM, with rat macrophages causes NO generation with up-regulation of iNOS expression on these cells. The data presented here show that the GXM concentration (250 μg ml^{-1}) which induced a significant increment in iNOS expression is high but still biologically relevant since GXM was detected

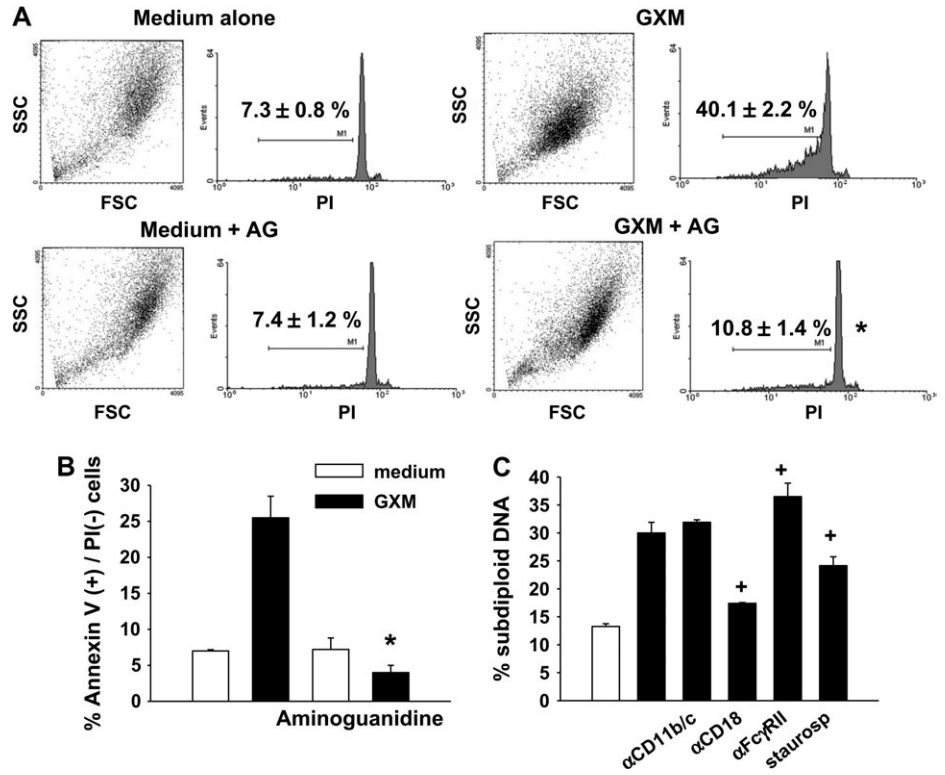

Fig. 7. GXM-induced apoptosis of peritoneal macrophages is dependent on NO production, CD18 interactions and PKC activation. Macrophages (10^6 ml^{-1}) were incubated for 48 h in the presence or absence of AG (2 mM) or GXM (250 μg). (A) Apoptosis was analyzed by flow cytometry after ethanol fixation and PI staining. Dot plots display forward scatter (FSC) versus side scatter (SSC) parameters, and histograms display DNA content by PI staining. Apoptotic cells appear as a sub-G_1 peak measured in the marker region (M1). The numbers indicate the mean ± SEM of the percentage of cells with subdiploid DNA content. (B) Annexin V–FITC binding and PI staining of unfixed cells. Bars indicate the mean ± SEM of the percentage of annexin V–FITC$^+$ PI$^-$ cells. *$P < 0.05$ (GXM-treated cells pre-incubated with AG versus GXM-treated cells). (C) Percentage of apoptosis measured as subdiploid DNA content by flow cytometry, after PI staining of macrophages incubated with or without GXM, in the presence or absence of mAbs to CD11b/c, CD18, FcγRII (10 μg ml^{-1}) or staurosporine. $^+P < 0.05$ (GXM-treated cells pre-incubated with staurosporine, mAbs to CD18 or FcγRII versus GXM-treated cells).

in the serum of patients at concentrations as high as 1 mg ml^{-1} (18). In agreement, in a recent publication by Villena *et al.* (27), it was reported that GXM induces NO production and iNOS expression in the RAW cell line.

Cryptococcus neoformans and *C. gattii* were classified into five capsular serotypes, which have considerable structural and antigenic diversity in the GXM (2, 17). Furthermore, increasing evidence confirms that these two species cause different clinical manifestation, thereby suggesting differences in the mechanisms of virulence (2). In the present study, GXM from serotype B *C. gattii* also promoted macrophage NO production, but to a lesser extent than GXM from serotype A *C. neoformans*. In a similar way, Yauch *et al.* (35) published differences in the capacity of GXMs isolated from all four cryptococcal serotypes to inhibit proliferation of activated PBMCs. Further investigations are necessary to perform in order to elucidate if these phenomena are related to the size or molecular structure differences of GXMs from *C. neoformans* and *C. gattii.*

A previous publication from our laboratory demonstrated that peritoneal macrophages from rats with disseminated cryptococcosis produce more than twice the amount of NO as peritoneal cells from uninfected rats (9). In the present work, we have shown that most peritoneal cells take up the polysaccharide after i.p. GXM injection (Fig. 4) and that these cells produce elevated nitrite levels after culture (Fig. 2). Moreover, data from Fig. 2 suggest a role of the intracellular kinase, PKC, in the NO produced by *in vivo* GXM-treated macrophages. In this sense, Zhou *et al.* (45) have published that PKC-dependent signaling pathway plays a major role in the enhancement of iNOS expression in LPS-stimulated rat peritoneal macrophages. The capacity of GXM to induce iNOS *in vivo* was confirmed by immunohistochemistry of lung tissue from GXM-injected rats. In a previous publication, we demonstrated that rats injected via i.c. with GXM showed a strong polysaccharide immunoreactivity and an increased number of apoptotic cells in the lungs, 7 days post-inoculation (30). Therefore, the elevated iNOS expression detected in lungs from the GXM-treated rats reported here coincides with the polysaccharide retention and the increased apoptosis level previously reported in these animals.

Our study further demonstrated that GXM-induced NO production involves engagement of CD18 on macrophages since the blocking of this integrin caused a decrease in NO synthesis. The CD18 complexes are heterodimeric integrins of the β2 (CD18) family composed of three members, CD11a/CD18 (LFA-1), CD11b/CD18 [Mac-1 or complement receptor 3 (CR3)] and CD11c/CD18 (CR4). On phagocytic

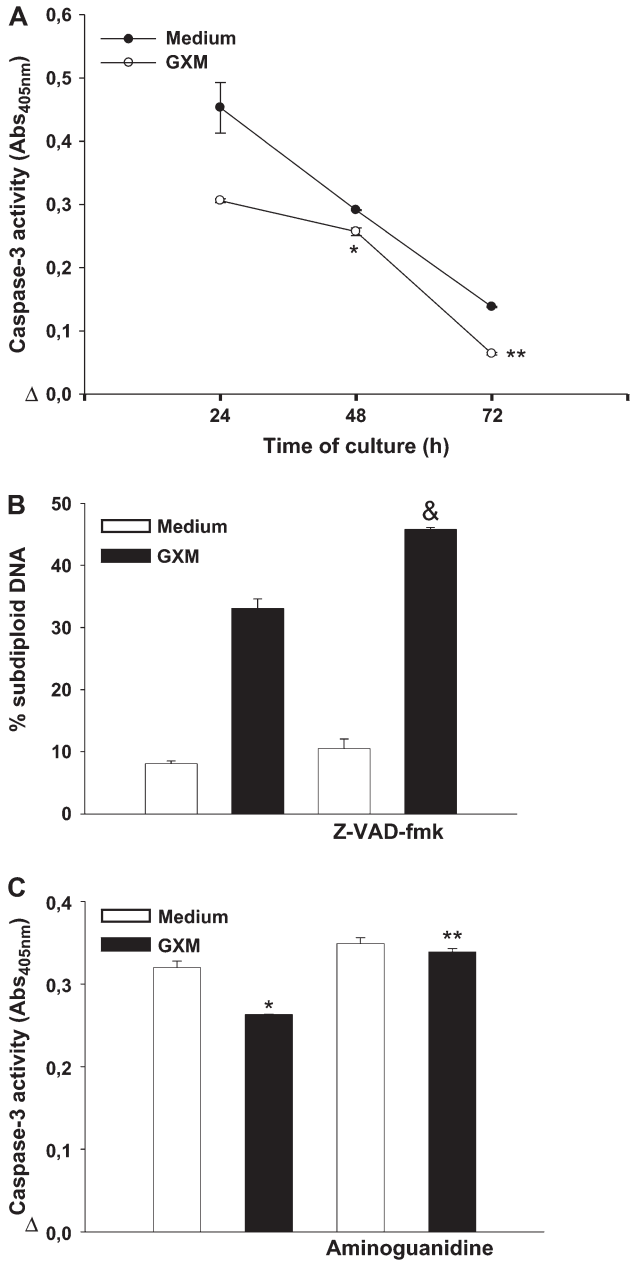

Fig. 8. GXM suppresses caspase-3 activity via NO generation and promotes a caspase-independent apoptosis. (A). Activation of caspase-3 activity. Macrophages (10^6) were incubated in medium alone or with GXM (250 μg ml^{-1}) for 24, 48 and 72 h of culture. The cells were lysed and centrifuged, and the supernatants were examined for caspase-3 activities by a colorimetric method. Optical density (OD) results were taken by subtracting the background OD at T_0 from the OD at 2 h of reaction. *$P < 0.05$ (GXM-treated versus -untreated cells). (B). Caspase-independent apoptosis. Macrophages were pre-incubated with 50 mM of Z-VAD-fmk in medium alone or with GXM for 48 h, and the apoptosis was determined by PI staining. *$P < 0.05$ (GXM-treated cells pre-incubated with Z-VAD-fmk versus GXM-treated cells). (C). NO participation in GXM-mediated caspase-3 activity inhibition. Macrophages were incubated in medium alone or with GXM in the absence or presence of AG for 24 h. Supernatants from cell lysates were examined for caspase-3 activities by a colorimetric method. *$P < 0.05$ (GXM-treated versus -untreated cells). **$P < 0.05$ (GXM and AG-treated versus AG-treated cells)

cells, CD18 associated with CD11b (CR3) or CD11c (CR4) is responsible for particle internalization (49). Some fungi may interact with both subunits of CR3, whereas others, like *Histoplasma capsulatum*, directly bind to CD18 (43). Dong and Murphy (21) first demonstrated that *C. neoformans* GXM bind to CD18 without interacting with CD11a or interfering with CD11b expression on human neutrophils. Later, Monari *et al.* (22, 42) also reported GXM–CD18 interactions on human and mouse macrophages. The data presented in this paper show that CD18, but not CD11b or CD11c, participated in GXM-induced NO synthesis or GXM macrophage accumulation. Furthermore, the CD11b subunit has a lectin-like domain that recognized mannose and β-glucans (43). The results presented here also show that GXM did not stimulated NO via mannose or β-glucan receptors. Moreover, it was previously published that these receptors are not involved in the immune response to GXM or encapsulated *C. neoformans* infections (50). The polysaccharide motifs that particularly interact with CD18 are still unknown, but xylose or glucuronic acid in the side chains found in the GXM structure (17) might be carbohydrates interacting with CD18. In the current work, the GXM-mediated NO production by rat macrophages was not modified in the presence of antibodies to TLR-2 or TLR-4. In contrast, it has been reported that treatment of human macrophages with GXM resulted in an increased expression of CD40 and CD86 via perturbation of TLR-4 (42). However, Nakamura *et al.* (51) published a limited contribution of TLRs to the host response to *C. neoformans*. Furthermore, the abrogation of GXM-induced NO synthesis by blocking CD18 was not complete, suggesting that other receptors could also be involved in this phenomenon. It has also been demonstrated that GXM-induced immune suppression was mediated by direct engagement of FcγRII (23). In agreement, in the present study, we observed that after blocking FcγRII, macrophages produced higher levels of NO in the presence of GXM than those observed in the absence of the anti-FcγRII antibody. Therefore, it seems probable that FcγRII in rat macrophages is also involved in the inhibitory signals triggered by GXM.

The signaling cascade coupling of CD18 is not well understood. However, it has been reported that engagement of CD18 induces activation of PKC, a serine/threonine kinase that exists as a family of different isotypes (49). CR3-mediated cell activation is sensitive to inhibitors of PKC, whereas it is not affected by inhibitors of tyrosine kinases (49). In this sense, the data presented here have shown that PKC, but not tyrosine kinase activation, is involved in GXM-induced NO synthesis by macrophages at the level of iNOS expression. Therefore, these results strongly suggest that the engagement of CD18 linked to PKC forms a pathway involved in macrophage stimulation by GXM. Taking into account that the activation of MAPK is involved in iNOS expression by different stimuli (45), we evaluated their participation in GXM-induced NO production. The results demonstrate the lack of involvement of MAPK activation in the GXM-induced NO release by macrophages since chemical inhibitors to p38 and ERK1/2 MAPK failed to block the increase in nitrite levels by GXM-stimulated macrophages. Coinciding with this, Shoham *et al.* (19) published that although GXM stimulates cells to translocate NF-κB to the nucleus in CHO cells, it does not activate MAPK.

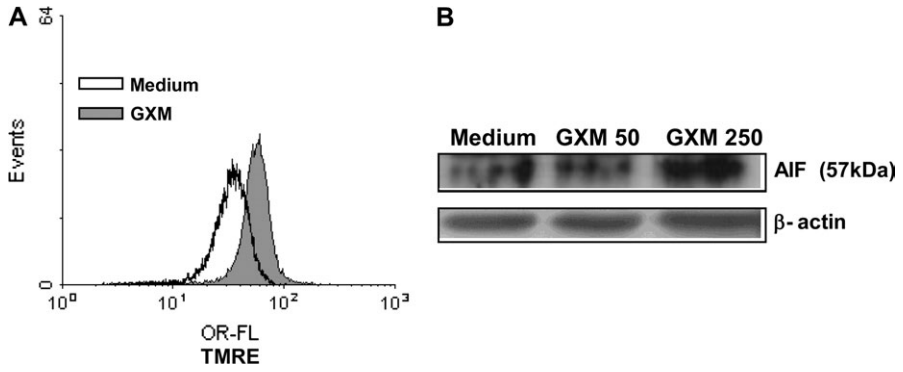

Fig. 9. Effects of GXM on mitochondrial integrity and cytosolic AIF expression. (A) Macrophages (10^6 ml^{-1}) were incubated in medium alone (shaded histogram) or with GXM (250 μg ml^{-1}, open histogram) for 48 h, and mitochondrial dysfunction was detected by staining with TMRE and flow cytometry analysis. (B) Cytosolic fractions from macrophages (10^6 ml^{-1}) in medium alone or treated with GXM (50 and 250 μg ml^{-1}) for 48 h were subjected to SDS-PAGE and probed with the appropriate antibodies. β-Actin was the loading control for the cytosolic fraction. Histograms and blots are representative of three independent experiments.

On the other hand, in the present study, we have observed that rat macrophages can efficiently internalize GXM in the absence of opsonins, with the polysaccharide showing a point-like attachment site, suggesting an aggregation of potential receptors or binding sites on macrophages. This pattern of GXM uptake has also been reported for mouse macrophages (24). Furthermore, concerning the pathways involved in NO generation, the data demonstrate that CD18, FcγRII and PKC were also mediating the GXM binding to macrophages. In this sense, it has been reported that PKC activation enhances CD18 expression and its ability to bind ligands (49), and human macrophages up-regulate CD18 after treatment with GXM (42). In contrast, the receptors or intracellular kinases were neither involved in NO generation nor mediated the macrophage GXM accumulation. In addition, the results did not show a strong correlation between the inhibition of GXM–FITC uptake and modulation of NO production after blocking CD18 or FcγRII. This could be due to that iNOS activation is a consequence of polysaccharide recognition by CD18 or FcγRII and other yet unknown receptors and might be independent on the subsequent amount of intracellular polysaccharide accumulation (52). On the other hand, Cobb *et al.* (53) discovered that NO produced by iNOS activation mediates the intracellular processing of some microbial polysaccharides through NO oxidation. However, it is unknown whether or not NO has any effect on the GXM structure or its processing by macrophages.

Several studies have demonstrated that pathogen-derived molecules can promote host cell apoptosis (12). Furthermore, a high output NO synthesis, such as that which occurs after the expression of iNOS, contributes to the induction of apoptosis in inflammatory cells and therefore to the resolution of the inflammation (13). In this study, we have demonstrated that GXM is able to induce macrophage apoptosis. Our data show that macrophages loaded with GXM underwent apoptosis since double immunofluorescence labeling revealed cells with cytoplasmic GXM detection and nuclei positive for the TUNEL reaction. Related to this, we previously published that tisular macrophages with intracellular storage of polysaccharide revealed apoptotic nuclei, during a disseminated cryptococcal infection in rats (28). The macrophage apoptosis observed in the current work occurred after 48 h of incubation with 250 μg of GXM and was abrogated by the iNOS inhibitor, AG, revealing that the main mechanism of cell death is by elevated NO production. Furthermore, as in the case of the pathways involved in GXM-mediated NO production, inhibition of CD18, FcγRII and PKC also modulated the GXM macrophage apoptosis. However, Villena *et al.* (27) recently published that GXM promotes mouse macrophage apoptosis through Fas–FasL interactions. In the present, we did not detect any increase in the Fas expression on macrophages incubated with GXM respect to macrophages in medium alone (data not shown). In addition, the iNOS inhibitor completely eliminated the apoptosis induced by the polysaccharide. The discrepancies between the mechanisms involved in GXM-mediated macrophage apoptosis reported here and those published by Villena *et al.* (27) could be due to the different serotypes used by these authors (*C. neoformans* serotype D) and to the functional differences between rat and mouse macrophages against cryptococcal components reported by Shao *et al.* (54). These authors found that rat macrophages have a greater phagocytosis and more oxidative and non-oxidative activities than mouse macrophages.

On the other hand, caspase activation is a hallmark of apoptosis and plays a critical role in the initiation and execution of this programmed cell death (46). Notably, however, mammalian caspases have also evolved additional roles in inflammatory responses (55–57). The differentiation of human monocytes to macrophages has also been shown to require caspase activation, which then participates in the cytoskeletical changes in terminal differentiation and could play a critical role in the ability of macrophages to form extensively modified structures, such as cell projections and giant cells (56). Mouse macrophages are known to spontaneously activate caspase-3 on adherence (57). In agreement with this, we observed that rat macrophages showed an increased caspase-3 activity, which was significantly reduced by the presence of GXM. NO also participated in this inhibitory effect since caspase-3 activity in macrophages incubated with GXM was restored in the presence of AG. These results coincide with the fact that NO is able to suppress caspase activity by *s*-nitrosilation of the cysteine at the catalytic site of

caspase (58). In addition, Wong *et al.* (55) demonstrated that caspase activity was partially controlled by the activity of iNOS, which is up-regulated during the maturation of dendritic cells. Thus, our data suggest that free cryptococcal polysaccharide interferes in the caspase activity of macrophages, which could be then critical for the optimal functioning of macrophages during fungal infection. Finally, we confirmed that GXM-mediated apoptosis is independent of caspase activation since the pan-caspase inhibitor Z-VAD-fmk did not restore the viability of GXM-stimulated macrophages.

It has been demonstrated that mitochondrial damage can lead to caspase-independent death through activation of death receptors, such as the AIF or Endo G (47). In particular, AIF is a principal executioner of pneumococcus- and group B streptococcus-induced macrophage apoptosis (34, 59). In the present work, we have demonstrated that GXM increases the mitochondrial membrane permeability and AIF cytosolic expression, suggesting a caspase-independent mitochondrial-mediated apoptosis triggered by GXM.

In conclusion, the NO-mediated apoptosis of macrophages promoted by high doses of free capsular polysaccharide of *C. neoformans* may represent a novel strategy of immunoevasion by interfering with the effector functions of the central cells in the host defense against this fungus. Moreover, the GXM-induced apoptosis of macrophages could contribute to limit host tissue damage during the infection.

Funding

Agencia Nacional de Promoción Científica y Tecnológica (PICT 33326); Consejo Nacional de Investigaciones Científicas y Técnicas de Argentina (PIP 6327); Secretaría de Ciencia y Tecnología, Universidad Nacional de Córdoba (Grant 2007).

Acknowledgements

J.L.B. and A.P.G. are PhD fellows of Consejo Nacional de Investigaciones Científicas y Técnicas and L.S.C. and D.T.M. are members of the Research Career of Consejo Nacional de Investigaciones Científicas y Técnicas. We would like to thank native speaker, Paul Hobson for revision of the manuscript.

Abbreviations

AG	aminoguanidine
AIF	apoptosis-inducing factor
ATCC	American Type Culture Collection
CR	complement receptor
CTAB	cetyltrimethyl ammonium bromide
DAB	diaminobenzidine
Endo G	endonuclease G
ERK	extracellular signal-regulated kinases
FBS	fetal bovine serum
FcγR II	Fcγ receptor II
GXM	glucuronoxylomannan
i.c.	intracardiac
iNOS	inducible nitric oxide synthase
i.p.	intra-peritoneal
MAPK	mitogen-activated protein kinase
MFI	mean fluorescence intensity
NF-κB	nuclear factor-kappa B
NO	nitric oxide
PB	polymixin B
PI	propidium iodide
PKC	protein kinase C
pNA	*p*-nitroanilide
TLR	Toll-like receptor
TMRE	tetramethylrhodamineethylester
TUNEL	TdT-mediated biotin–dUTP nick-end labeling
Z-VAD-fmk	N-Benzyloxycarbonyl-Val-Ala-Asp(O-Me) fluoromethyl ketone

References

1 Feldmesser, M., Kress, Y., Novikoff, P. and Casadevall, A. 2000. *Cryptococcus neoformans* is a facultative intracellular pathogen in murine pulmonary infection. *Infect. Immun.* 68:4225.
2 Perfect, J. R. and Chayakulkeeree, M. 2006. Cryptococcosis. *Infect. Dis. Clin. North Am.* 20:507.
3 Garcia-Hermoso, D., Janbon, G. and Dromer, F. 1999. Epidemiological evidence for dormant *Cryptococcus neoformans* infection. *J. Clin. Microbiol.* 37:3204.
4 Goldman, D., Lee, S. C. and Casadevall, A. 1994. Pathogenesis of pulmonary *Cryptococcus neoformans* infection in the rat. *Infect. Immun.* 62:4755.
5 MacMicking, J., Xie, Q. W. and Nathan, C. 1997. Nitric oxide and macrophage function. *Annu. Rev. Immunol.* 15:323.
6 Gonzalez, A., de Gregori, W., Velez, D., Restrepo, A. and Cano, L. E. 2000. Nitric oxide participation in the fungicidal mechanism of gamma interferon-activated murine macrophages against *Paracoccidioides brasiliensis* conidia. *Infect. Immun.* 68:2546.
7 Gobert, A. P., Mersey, B. D., Cheng, Y., Blumberg, D. R., Newton, J. C. and Wilson, K. T. 2002. Urease release by *Helicobacter pylori* stimulates macrophage inducible nitric oxide synthase. *J. Immunol.* 168:6002.
8 Magez, S., Radwanska, M., Drennan, M. *et al.* 2007. Tumor necrosis factor (TNF) receptor-1 (TNFp55) signal transduction and macrophage-derived soluble TNF are crucial for nitric oxide-mediated *Trypanosoma congolense* parasite killing. *J. Infect. Dis.* 196:954.
9 Rossi, G. R., Cervi, L. A., Garcia, M. M., Chiapello, L. S., Sastre, D. A. and Masih, D. T. 1999. Involvement of nitric oxide in protecting mechanism during experimental cryptococcosis. *Clin. Immunol.* 90:256.
10 Wu-Hsieh, B. A., Chen, W. and Lee, H. J. 1998. Nitric oxide synthase expression in macrophages of *Histoplasma capsulatum*-infected mice is associated with splenocyte apoptosis and unresponsiveness. *Infect. Immun.* 66:5520.
11 Albina, J. E., Cui, S., Mateo, R. B. and Reichner, J. S. 1993. Nitric oxide-mediated apoptosis in murine peritoneal macrophages. *J. Immunol.* 150:5080.
12 Lüder, C. G. K., Gross, U. and Lopes, M. F. 2001. Intracellular protozoan parasites and apoptosis: diverse strategies to modulate parasite-host interactions. *Trends Parasitol.* 17:480.
13 Taylor, E. L., Megson, I. L., Haslett, C. and Rossi, A. G. 2003. Nitric oxide: a key regulator of myeloid inflammatory cell apoptosis. *Cell Death Differ.* 10:418.
14 Strasser, A., O'Connor, L. and Dixit, V. M. 2000. Apoptosis signaling. *Annu. Rev. Biochem.* 69:217.
15 Jaattela, M. and Tschopp, J. 2003. Caspase-independent cell death in T lymphocytes. *Nat. Immunol.* 4:416.
16 Cande, C., Cecconi, F., Dessen, P. and Kroemer, G. 2002. Apoptosis-inducing factor (AIF): key to the conserved caspase-independent pathways of cell death? *J. Cell Sci.* 115:4727.
17 Cherniak, R., Valafar, H., Morris, L. C. and Valafar, F. 1998. *Cryptococcus neoformans* chemotyping by quantitative analysis of ^{1}H nuclear magnetic resonance spectra of glucuronoxylomannans with a computer-simulated artificial neural network. *Clin. Diagn. Lab. Immunol.* 5:146.
18 Brouwer, A. E., Teparrukkul, P., Pinpraphaporn, S. *et al.* 2005. Baseline correlation and comparative kinetics of cerebrospinal fluid colony-forming unit counts and antigen titers in cryptococcal meningitis. *J. Infect. Dis.* 192:681.
19 Shoham, S., Huang, C., Chen, J., Golenbock, D. T. and Levitz, S. M. 2001. Toll-like receptor 4 mediates intracellular signaling without TNF-α release in response to *Cryptococcus neoformans* polysaccharide capsule. *J. Immunol.* 166:4620.

20 Yauch, L. E., Mansour, M. K. and Levitz, S. M. 2005. Receptor-mediated clearance of *Cryptococcus neoformans* capsular polysaccharide *in vivo*. *Infect. Immun.* 73:8429.

21 Dong, Z. M. and Murphy, J. W. 1997. Cryptococcal polysaccharides bind to CD18 on human neutrophils. *Infect. Immun.* 65:557.

22 Monari, C., Pericolini, E., Bistoni, F., Casadevall, A., Kozel, T. R. and Vecchiarelli, A. 2005. *Cryptococcus neoformans* capsular glucuronoxylomannan induces expression of fas ligand in macrophages. *J. Immunol.* 174:3461.

23 Monari, C., Kozel, T. R., Paganelli, F. *et al.* 2006. Microbial immune suppression mediated by direct engagement of inhibitory Fc receptor. *J. Immunol.* 177:6842.

24 Chang, Z. L., Netski, D., Thorkildson, P. and Kozel, T. R. 2006. Binding and internalization of glucuronoxylomannan, the major capsular polysaccharide of *Cryptococcus neoformans*, by murine peritoneal macrophages. *Infect. Immun.* 74:144.

25 Goldman, D., Youngsoo, C., Meng-liang, Z., Casadevall, A. and Lee, S. C. 1996. Expression of inducible nitric oxide synthase in rat pulmonary *Cryptococcus neoformans* granulomas. *Am. J. Pathol.* 148:1275.

26 Goldman, D. L., Lee, S. C., Mednick, A. J., Montella, L. and Casadevall, A. 2000. Persistent *Cryptococcus neoformans* pulmonary infection in the rat is associated with intracellular parasitism, decreased inducible nitric oxide synthase expression, and altered antibody responsiveness to cryptococcal polysaccharide. *Infect. Immun.* 68:832.

27 Villena, S., Pinheiro, R., Pinheiro, C. S. *et al.* 2008. Capsular polysaccharides galactoxylomannan and glucuronoxylomannan from *Cryptococcus neoformans* induce macrophage apoptosis mediated by Fas ligand. *Cell. Microbiol.* 10:1274.

28 Chiapello, L. S., Aoki, M. P., Rubinstein, H. R. and Masih, D. T. 2003. Apoptosis induction by glucuronoxylomannan of *Cryptococcus neoformans*. *Med. Mycol.* 41:347.

29 Chiapello, L., Iribarren, P., Cervi, L., Rubinstein, H. and Masih, D. T. 2001. Mechanisms for induction of immunosuppression during experimental cryptococcosis. Role of glucuronoxylomannan. *Clin. Immunol.* 100:96.

30 Chiapello, L. S., Baronetti, J. L., Aoki, M. P., Rubinstein, H. R. and Masih, D. T. 2004. Immunosuppression, interleukin-10 synthesis and apoptosis are induced in rats inoculated with *Cryptococcus neoformans* glucuronoxylomannan. *Immunology* 113:392.

31 Dubois, M., Gilles, K. A., Hamilton, J. K., Rebers, P. A. and Smith, F. 1956. Colorimetric method for determination of sugars and related substances. *Anal. Chem.* 28:350.

32 Prigent-Richard, S., Cansell, M., Vassy, J. *et al.* 1998. Fluorescent and radiolabeling of polysaccharides: binding and internalization experiments on vascular cells. *J. Biomed. Mater. Res.* 40:275.

33 Sedgwick, J. B., Shikama, Y., Nagata, M., Brener, K. and Busse, W. W. 1996. Effect of isolation protocol on eosinophil function: Percoll gradients versus immunomagnetic beads. *J. Immunol. Methods* 198:15.

34 Fettucciari, K., Fetriconi, I., Mannucci, R. *et al.* 2006. Group B *Streptococcus* induces macrophage apoptosis by calpain activation. *J. Immunol.* 176:7542.

35 Yauch, L. E., Lam, J. S. and Levitz, S. M. 2006. Direct inhibition of T-cell responses by the *Cryptococcus* capsular polysaccharide glucuronoxylomannan. *PLoS Pathog.* 2:e120.

36 Kerr, J. F. R., Wyllie, A. H. and Currie, A. R. 1972. Apoptosis: a basic biological phenomenon with wide-ranging implications in tissue kinetics. *Br. J. Cancer* 26:239.

37 Nicoletti, I., Migliorati, M., Pagliacci, M., Grignani, F. and Riccardi, C. A. 1991. Rapid and simple method for measuring thymocyte apoptosis by propidium iodide staining and flow cytometry. *J. Immunol. Methods* 139:271.

38 Martin, S. J., Reutelingsperger, C. P., McGahon, A. J. *et al.* 1995. Early redistribution of plasma membrane phosphatidylserine is a general feature of apoptosis regardless of the initiating stimulus: inhibition by overexpression of Bcl-2 and Abl. *J. Exp. Med.* 182:1545.

39 Berro, A. I., Perry, G. A. and Agrawal, D. K. 2004. Increased expression and activation of CD30 induce apoptosis in human blood eosinophils. *J. Immunol.* 173:2174.

40 Jayaraman, S. 2005. Flow cytometric determination of mitochondrial membrane potential changes during apoptosis of T lymphocytic and pancreatic beta cell lines: comparison of tetramethylrhodamineethylester (TMRE), chloromethyl-X-rosamine (H2-CMX-Ros) and MitoTracker Red 580 (MTR580). *J. Immunol. Methods* 306:68.

41 Takai, N., Kataoka, M., Higuchi, Y., Matsuura, K. and Yamamoto, S. 1997. Primary structure of rat CD14 and characteristics of rat CD14, cytokine, and NO synthase mRNA expression in mononuclear phagocyte system cells in response to LPS. *J. Leukoc. Biol.* 61:736.

42 Monari, C., Bistoni, F., Casadevall, A. *et al.* 2005. Glucuronoxylomannan, a microbial compound, regulates expression of costimulatory molecules and production of cytokines in macrophages. *J. Infect. Dis.* 191:127.

43 Taborda, C. and Casadevall, A. 2002. CR3 (CD11b/CD18) and CR4 (CD11c/CD18) are involved in complement-independent antibody-mediated phagocytosis of *Cryptococcus neoformans*. *Immunity* 16:791.

44 Vecchiarelli, A. 2000. Immunoregulation by capsular components of *Cryptococcus neoformans*. *Med. Mycol.* 38:407.

45 Zhou, X., Yang, W. and Li, J. 2006. Ca^{2+}- and protein kinase C-dependent signaling pathway for nuclear factor-κB activation, inducible nitric-oxide synthase expression, and tumor necrosis factor-α production in lipopolysaccharide-stimulated rat peritoneal macrophages. *J. Biol. Chem.* 281:31337.

46 Earnshaw, W. C., Martins, L. M. and Kauffmann, S. H. 1999. Mammalian caspases: structure, activation, substrates, and functions during apoptosis. *Annu. Rev. Biochem.* 68:383.

47 Leist, M. and Jäättelä, M. 2001. Four deaths and a funeral: from caspases to alternative mechanisms. *Nat. Rev. Mol. Cell Biol.* 2:589.

48 Lee, S. C., Dickson, D. W., Brosnan, C. F. and Casadevall, A. 1994. Human astrocytes inhibit *Cryptococcus neoformans* growth by a nitric oxide-mediated mechanism. *J. Exp. Med.* 180:365.

49 Chimini, G. and Chavrierni, P. 2000. Function of Rho family proteins in actin dynamics during phagocytosis and engulfment. *Nat. Cell Biol.* 2:191.

50 Nakamura, K., Kinjo, T., Saijo, S. *et al.* 2007. Dectin-1 is not required for the host defense to *Cryptococcus neoformans*. *Microbiol. Immunol.* 51:1115.

51 Nakamura, K., Miyagi, Y., Koguchi, Y. *et al.* 2006. Limited contribution of Toll-like receptor 2 and 4 to the host response to a fungal infectious pathogen, *Cryptococcus neoformans*. *FEMS Immunol. Med. Microbiol.* 47:148.

52 Lull, C., Wichers, H. and Savelkoul, H. F. 2005. Antiinflammatory and immunomodulating properties of fungal metabolites. *Mediat. Inflamm.* 2:63.

53 Cobb, B. A., Wang, Q., Tzianabos, A. O. and Kasper, D. L. 2004. Polysaccharide processing and presentation by the MHCII pathway. *Cell* 117:677.

54 Shao, X., Mednick, A., Alvarez, M., van Rooijen, N., Casadevall, A. and Goldman, D. L. 2005. An innate immune system cell is a major determinant of species-related susceptibility differences to fungal pneumonia. *J. Immunol.* 175:3244.

55 Wong, S. H., Santambrogio, L. and Strominger, J. L. 2004. Caspases and nitric oxide broadly regulate dendritic cell maturation and surface expression of class II MHC proteins. *Proc. Natl Acad. Sci. USA* 101:17783.

56 Sordet, O., Rebe, C., Penchette, S. *et al.* 2002. Specific involvement of caspases in the differentiation of monocytes into macrophages. *Blood* 100:4446.

57 Nhan, T. Q., Liles, W. C. and Schwartz, S. M. 2005. Role of caspases in death and survival of the plaque macrophage. *Arterioscler. Thromb. Vasc. Biol.* 25:895.

58 Kim, K., Kim, P. K. M., Kwon, Y., Bai, S., Nam, W. and Kim, Y. M. 2002. Regulation of apoptosis by nitrosative stress. *J. Biochem. Mol. Biol.* 35:127.

59 Braun, J. S., Novak, P. J., Murray, C. M. *et al.* 2001. Apoptosis-inducing factor mediates microglial and neuronal apoptosis caused by pneumococcus. *J. Infect. Dis.* 184: 1300.